

Published in final edited form as:

Mol Carcinog. 2010 May ; 49(5): 450–463. doi:10.1002/mc.20616.

Grape Seed Proanthocyanidin Suppression of Breast Cell Carcinogenesis Induced by Chronic Exposure to Combined 4-(Methylnitrosamino)-1-(3-Pyridyl)-1-Butanone and Benzo[a]Pyrene

Xiaoyu Song^{1,2}, Nalin Siriwardhana¹, Kusum Rathore^{1,3}, Degui Lin², and Hwa-Chain Robert Wang^{1,3,*}

¹Department of Comparative Medicine, College of Veterinary Medicine, University of Tennessee, Knoxville, Tennessee

²College of Veterinary Medicine, China Agricultural University, Beijing, PR China

³Graduate School of Genome Science and Technology, University of Tennessee, Knoxville, Tennessee

Abstract

Breast cancer is the most common type of cancer among women in northern America and northern Europe; dietary prevention is a cost-efficient strategy to reduce the risk of this disease. To identify dietary components for the prevention of human breast cancer associated with long-term exposure to environmental carcinogens, we studied the activity of grape seed proanthocyanidin extract (GSPE) in suppression of cellular carcinogenesis induced by repeated exposures to low doses of environmental carcinogens. We used combined carcinogens 4-(methylnitrosamino)-1-(3-pyridyl)-1-butanone (NNK) and benzo[a]pyrene (B[a]P), at picomolar concentrations, to repeatedly treat noncancerous, human breast epithelial MCF10A cells to induce cellular acquisition of cancer-related properties of reduced dependence on growth factors, anchorage-independent growth, and acinar-conformational disruption. Using these properties as biological target endpoints, we verified the ability of GSPE to suppress combined NNK- and B[a]P-induced precancerous cellular carcinogenesis and identified the minimal, noncytotoxic concentration of GSPE required for suppressing precancerous cellular carcinogenesis. We also identified that hydroxysteroid-11-beta-dehydrogenase 2 (HSD11B2) may play a role in NNK- and B[a]P-induced precancerous cellular carcinogenesis, and its expression may act as a molecular target endpoint in GSPE's suppression of precancerous cellular carcinogenesis. And, the ability of GSPE to reduce gene expression of cytochrome-P450 enzymes CYP1A1 and CYP1B1, which can bioactivate NNK and B[a]P, possibly contributes to the preventive mechanism for GSPE in suppression of precancerous cellular carcinogenesis. Our model system with biological and molecular target endpoints verified the value of GSPE for the prevention of human breast cell carcinogenesis induced by repeated exposures to low doses of multiple environmental carcinogens.

Keywords

breast cancer; dietary prevention; environmental carcinogens; target endpoints

© 2010 WILEY-LISS, INC.

*Correspondence to: Department of Comparative Medicine, College of Veterinary Medicine, University of Tennessee, 2407 River Drive, Knoxville, TN 37996.

X. Song and N. Siriwardhana contributed equally to this work.

INTRODUCTION

Epidemiologic and experimental evidence suggests that dietary polyphenolic compounds, which are widely found in vegetables, fruits, and tea, possess anticancer, antiproliferative, apoptotic, and other activities that inhibit bioactivating enzymes and induce detoxifying enzymes [1]. Within the superfamily of polyphenolic compounds are proanthocyanidins, which are enriched in grape seeds and are oligomers and polymers of the catechin family [2]. Grape seed proanthocyanidin extract (GSPE) has been shown to exhibit antioxidant and anticancer activities in both in vitro and in vivo models [3–6]; for example, it shows some diet-dependent, chemo-preventive activity in a rat model with mammary cancer induced by 7,12-dimethylbenz[a]anthracene (DMBA) [6]. Whether dietary GSPE is able to prevent the breast cell carcinogenesis associated with chronic exposures to environmental carcinogens is not clear.

Growing evidence indicates that exposure to environmental carcinogens may increase the risk of sporadic human breast cancer [7–11]. Carcinogenesis of human breast cells to become precancerous and cancerous is a multiyear, multistep, and multipath process with progressive genetic and epigenetic alterations [7]. Ductal carcinoma in situ (DCIS) formation predicts the substantial likelihood of developing breast cancer, and breast cells involved in DCIS are precancerous [12,13]. Thus, it is important to understand the nature of long-term, accumulative exposure to environmental carcinogens in the development of DCIS, which can be used as a target endpoint for early, precancerous prevention of human breast cell carcinogenesis.

We have tested a cellular model that is able to reveal the potency of an environmental carcinogen to induce chronic carcinogenesis of breast cells to progressively acquire identifiable cancer-related properties, mimicking long-term exposure of breast cells to low doses of an environmental carcinogen [14–16]. In the studies, repeated exposure of immortalized, noncancerous, human breast epithelial MCF10A cells to benzo[a]pyrene (B[a]P) or 4-(methylnitrosamino)-1-(3-pyridyl)-1-butanone (NNK) at picomolar concentrations, which can be detected in body fluids and tissues of cancer patients and tobacco users [17–19], results in induction of increasing acquisition of cancer-related cellular properties [15,16]. B[a]P, a family member of poly-cyclic aromatic hydrocarbons, is considered an environmental, tobacco, and dietary carcinogen [7,9,11,20,21], and it is identified as a mammary carcinogen in rodents [9,22]. B[a]P may contribute to human breast cancer development by its metabolites forming strong DNA adducts, causing DNA lesions [9,11,20]. However, B[a]P-derived DNA adducts alone are insufficient for inducing human breast cancer [7,20,23]. Our model verified the ability of B[a]P at 100 pM to chronically induce MCF10A cells to progressively acquire cancer-related properties of reduced dependence on growth factors, anchorage-independent growth, and acinar-conformational disruption, but not tumorigenicity [15]. NNK is regarded as an environmental and tobacco-specific carcinogen that causes lung cancer; however, gavage of rodents with NNK also results in the formation of DNA adducts in the mammary gland [24]. Using our model, we revealed that accumulated exposures of MCF10A cells to NNK at 100 pM are also able to induce cancer-related properties of reduced dependence on growth factors, anchorage-independent growth, and acinar-conformational disruption, but not tumorigenicity [16]. Possibly, NNK is able to act as a “precancerous mammary carcinogen” in the development of human breast cancer through long-term, accumulated exposure of breast cells to NNK. Our model reveals the ability of a carcinogen to induce cellular acquisition of cancer-related properties, which can be used as biological target endpoints for identifying bioactive components to suppress cellular carcinogenesis for early prevention of human breast cancer associated with long-term exposure to environmental carcinogens.

Using carcinogenesis-associated acquisition of cancer-related properties as biological target endpoints, we revealed the ability of GSPE at a maximal, noncytotoxic concentration to suppress precancerous carcinogenesis induced by a single carcinogen NNK in MCF10A cells [16]. In this report, we furthered our investigation to reveal the minimal, noncytotoxic concentration of GSPE required for suppressing chronic, precancerous cellular carcinogenesis induced by combined NNK and B[a]P. We also investigated molecular target endpoints and potential mechanism for GSPE in suppression of cellular carcinogenesis. We found that hydroxysteroid-11-beta-dehydrogenase 2 (HSD11B2) may play a role in NNK- and B[a]P-induced cellular acquisition of cancer-related properties and may act as a molecular target endpoint for GSPE in suppression of cellular carcinogenesis. The noncytotoxic, preventive mechanism for GSPE in suppression of NNK- and B[a]P-induced cellular carcinogenesis may involve reduction of bioactivating enzymes cytochrome-P450 1A1 (CYP1A1) and 1B1 (CYP1B1) contents.

MATERIALS AND METHODS

Cell Cultures, Reagents, and Cellular Carcinogenesis

MCF10A (American Type Culture Collection [ATCC], Rockville, MD) and derived cell lines were maintained in complete MCF10A (CM) medium (1:1 mixture of DMEM and HAM's F12, supplemented with mitogenic additives including 100 ng/mL cholera enterotoxin, 10 mg/mL insulin, 0.5 mg/mL hydro-cortisol, 20 ng/mL epidermal growth factor, and 5% horse serum) [14–16,25]. Human breast adenocarcinoma MCF7 cells were maintained in DMEM supplemented with 10% heat-inactivated fetal bovine serum. All cultures were maintained in medium supplemented with 100 U/mL penicillin and 100 mg/mL streptomycin in 5% CO₂ at 37°C. Stock aqueous solutions of NNK (Chemsyn, Lenexa, KS) and B[a]P (Aldrich, Milwaukee, WI) were prepared in dimethyl sulfoxide, which was used as a vehicle agent, and diluted with culture medium. GSPE (IH636, InterHealth Nutraceuticals, Benicia, CA), which contains 74% proanthocyanidins, was prepared in H₂O and diluted with culture medium.

Protocol for Inducing Chronic Carcinogenesis

Twenty-four hours after each subculturing, MCF10A cells were treated with combined NNK and B[a]P each at 100 pM in the absence and presence of 40 mg/mL GSPE for 48 h as one cycle of exposure for 5, 10, 15, and 20 cycles; cultures were subcultured every 3 d (3 d/cycle) [15,16]. After exposures to carcinogens and GSPE, cells were assayed to detect survived cell populations that acquired the cancer-related properties of a reduced dependence on growth factors, anchorage-independent growth, and acinar-conformational disruption.

Assay for Acquisition of Reduced Dependence on Growth Factors

The low-mitogen (LM) medium contained reduced total serum and mitogenic additives to 2% of the concentration formulated in CM medium as described above [15,16]. Cells were seeded in LM medium and maintained in 5% CO₂ at 37°C. Growing cell colonies that reached 0.5 mm diameter in 10 d were identified as cell clones acquiring the cancer-related property of a reduced dependence on growth factors.

Assay for Acquisition of Anchorage-Independent Growth

The base layer consisted of 2% low-gelling, SeaPlaque agarose (Sigma–Aldrich, St. Louis, MO) in CM medium. Then, soft-agar consisting of 0.4% SeaPlaque agarose in a mixture (1:1) of CM medium with 3-d conditioned medium prepared from MCF10A cultures was mixed with cells and plated on top of the base layer in 60 mm diameter culture dishes [14–

16]. Cultures were maintained in 5% CO₂ at 37°C. Growing colonies that reached 0.1 mm diameter by 20 d were identified as cell clones acquiring the cancer-related property of anchorage-independent growth.

Assay for Acquisition of Acinar-Conformational Disruption

Placed as a Matrigel base of reconstituted basement membrane in each well of 24-well culture plates were 400 µL of Growth Factor-Reduced Matrigel Matrix (BD Biosciences, Bedford, MA) [15,16,26]. 2×10^3 cells were mixed with CM medium containing 4% Matrigel and plated on top of the base layer of Matrigel. Cultures were maintained in 5% CO₂ at 37°C and were replaced with fresh CM medium containing 2% Matrigel every 3 d for 14 d.

Spheroids in Matrigel were collected and overlaid with 5% agarose; then blocks of agarose-packed Matrigel spheroids were fixed in neutral-buffered formalin and embedded in paraffin for histological examination of 5 mm H&E-stained sections.

Assay for Cell Growth and Viability

A methyl thiazolyl tetrazolium (MTT) assay kit (ATCC) was used to measure cell growth and viability in cultures [15,16]. As described by the manufacturer, cells were seeded into each well of 96-well culture plates for 24 h. After treatments, cells were incubated with MTT reagent for 4 h, followed by incubation with detergent reagent for 24 h. Quantification of reduced MTT reagent in cultures was determined with an enzyme-linked immunosorbent assay (ELISA) reader (Bio-Tek, Winooski, VT) at 570 nm.

Tumorigenic Assay

Cells were prepared with Matrigel basement membrane matrix (13.35 mg/mL; BD Biosciences), and 1×10^7 cells in 100 µL were injected subcutaneously into flanks of 5-wk-old, female, athymic NCr-nu/nu mice (NCI, Frederick, MD) [14]. Four mice were used per group and maintained under pathogen-free conditions, and mice were monitored weekly for 6 mo. All animal procedures were approved by The University of Tennessee Animal Care and Use Committee and were in accordance with the Public Health Service Policy on Humane Care and Use of Laboratory Animals (2002).

Study of Gene Expression With cDNA Microarrays

Total RNA was isolated from cultures using the Absolutely RNA kit (Stratagene, La Jolla, CA). For each sample, 15 µg of RNA was reverse transcribed to cDNA and labeled with either Cy3 or Cy5 using the CyScribe First-Strand cDNA Labeling Kit (Amersham, Piscataway, NJ). Cy3- and Cy5-labeled cDNA products were purified with the CyScribe GFX Purification Kit (Amersham). Reciprocal Cy3- and Cy5-labeled cDNA probes were prepared from target carcinogen-transformed cultures and reference parent counterpart cultures. The reverse dye labeling of cDNA probes accounted for dye-gene labeling bias. The Cy3- and Cy5-labeled cDNA mixture was heated and cohybridized onto a set of human 19K ESTs microarrays containing 19 008 characterized and unknown expressed sequence tags (Microarray Centre, SS-H19Kv7; University Health Network, Toronto, Ontario, Canada) at 37°C for 15 h. Microarrays were then washed with 1× SSC, 1× SSC/0.1% SDS, 1× SSC, and 0.1× SSC orderly. Hybridized microarrays were scanned in a GenePix 4000B scanner (Axon Instruments, Union City, CA). Using GenePix Pro analysis software 5.1 and Arrayvision 4.0 (Axon Instruments), fluorescence intensities for both channels were determined with a Cy3/Cy5 hybridization ratio across the arrays of 1. Each gene expression was determined after median background subtraction. Gene arrays with features that were either defective or unidentified were flagged and excluded. Gene arrays with features having

intensity ≥ 100 with signal over the local background in both channels were included. All experiments were performed with duplicates. As a technique control, cDNA probes were prepared from two independent parent cultures and were hybridized against each other on microarrays to reveal nonspecific changes in gene expression that were excluded from the final results. The log ratios from microarrays hybridized with reciprocally labeled cDNA probes were averaged to identify gene expression in target cells that was up or downregulated over counterpart expression in reference cells (one-way ANOVA at $P < 0.05$). Data analysis was performed using the GeneSifter system (VizX Labs LLC, Seattle, WA), a Web-based microarray data analysis system with weekly updated gene annotations, that is capable of assessing array quality, producing data clustering, and creating pathway and gene ontology reports.

Real-Time Quantitative Polymerase Chain Reaction (RTqPCR)

As described previously [15,16], the primers were designed with PrimerExpress software (Applied Bio-systems, Foster City, CA) to have amplicons of approximate 70–100 bp for each gene. The *TATA box-binding protein (TBP)* gene was used as an internal reference [27]. Primers of the target and reference genes were designated *HSD11B2* (forward: 5'-GTCTCTTGACTGGCTCAAGAATTAGG-3'; reverse: 5'-GTGGCAATTGGGAAGTACAGTACAT-3') and *TBP* (forward: 5'-GCCCGAAACGCCGAATAT-3'; reverse: 5'-CCGTGGTTCGTGGCTCTCT-3'). Total RNAs were isolated by the Absolutely RNA kit (Stratagene), and cDNAs were prepared using an iScript cDNA synthesis kit (Bio-Rad, Hercules, CA). Reactions were performed with a cDNA template of serially diluted concentrations on an ABI7000 Sequence Detection System (Applied Biosystems) using an iTaQ SYBR Green Supermix with Rox (Bio-Rad) to evaluate the amount of double-stranded DNA. The C_t numbers were extracted with ABI Prism 7000 SDS software with an auto baseline and appropriate manual C_t . The $2^{-\Delta\Delta C_t}$ and standard curve method were used to calculate the relative abundance of gene expression [28]. Statistical analysis was performed with a multiple regression model to initially normalize the C_t number for each target gene with the *TBP* gene, and subsequently to compare the target and reference normalized C_t [29]. The model estimated the intercept of the multiple standard curves to render a P -value and standard error for the $\Delta\Delta C_t$, which in turn was used to determine the ratio for relative gene expression with the formula of $2^{-\Delta\Delta C_t}$.

RNA Interference

Validated *HSD11B2*-specific siRNAs (sc-41379) and control siRNAs (sc-37007) were purchased from Santa Cruz Biotechnology (Santa Cruz, CA); *HSD11B2*-specific siRNAs are a pool of three target-specific 19–25 nt siRNAs designed to knock down gene expression. Cells in 35-mm culture dishes were transfected with 1 μ g of validated, *HSD11B2*-specific siRNAs and control siRNAs using siRNA transfection reagent (Santa Cruz Biotechnology).

Western Immunoblotting

Cells were lysed in a buffer (10 mM Tris-HCl, 150 mM NaCl, 1% Triton X-100, 5 mM EDTA, 10 mM sodium pyrophosphate, 10% glycerol, 0.1% Na_3VO_4 , 50 mM NaF, pH 7.4); cell lysates were isolated from the supernatants after centrifugation of crude lysates at 20 000g for 20 min [15,16]. Protein concentration in cell lysates was measured using the BCA assay (Pierce, Rockford, IL). Equal amounts of cellular proteins were resolved by electrophoresis in 10% SDS-polyacrylamide gels for Western immunoblotting with specific antibodies to *HSD11B2* and β -actin (Cell Signaling, Beverly, MA). Antigen-antibody complexes on filters were detected by the Supersignal chemiluminescence kit (Pierce).

Reverse Transcription PCR

One microgram of total RNA isolated from cultures using the Absolutely RNA kit (Stratagene) was reverse transcribed to cDNA using a Verso cDNA Kit (Thermo Scientific, Waltham, MA). The resulting cDNAs were subjected to PCR for CYP1A1 (forward: 5'-CCTGCTAGGGTTAGGAGGTC-3'; reverse: 5'-GCTCAGCCTAGTTCAAGCAG-3'), CYP1B1 (forward: 5'-CTAAGCTGTGTCTGCCCAAT-3'; reverse: 5'-CTTTTCCAAACAGCTTCCAA-3'), and β -actin (forward: 5'-GGACTTCGAGCAAGAGATGG-3'; reverse: 5'-AGCACTGTGTTGGCGTACAG-3'). PCR was carried out as follows: 1 cycle at 95°C for 2 min, 30 cycles at 95°C for 30 s, and 55°C for 45 s, and the final extension of 1 cycle at 72°C for 30 s. PCR products were electrophoresed on 2% agarose gel and visualized after ethidium bromide staining.

RESULTS

GSPE Suppression of Carcinogen-Induced Acquisition of Reduced Dependence on Growth Factors

A lack of growth factors causes normal cells to become growth-arrested in the cell cycle and to commit apoptosis; however, aberrantly increased cell survivability acquired to reduce dependence on growth factors can lead cells to tumorigenic transformation [30–32]. We have shown that repeated exposures of noncancerous breast epithelial MCF10A cells to a low dose of individual NNK and B[a]P at 100 pM resulted in progressive acquisition of the cancer-related ability of reduced dependence on growth factors [15,16]. To detect whether repeated exposures of cells to combined NNK and B[a]P will synergistically or additively induce cellular acquisition of cancer-related properties, MCF10A cells were exposed to individual or combined NNK and B[a]P each at 100 pM for 5, 10, 15, and 20 cycles. Exposures of MCF10A cells to combined NNK and B[a]P for 5, 10, 15, and 20 cycles resulted in cell lines NB-P5, -P10, -P15, and -P20, respectively. As shown in Figure 1A, repeated exposures of MCF10A cells to combined NNK and B[a]P for 5 cycles resulted in detectable increases of cell clones acquiring cancer-related ability of reduced dependence on growth factors, and 10 and 15 cycles of exposure resulted in significant and progressive increases of cell clones acquiring the reduced dependence on growth factors; however, additional exposures to combined NNK and B[a]P for a total of 20 cycles did not result in any additional increases of cell clones acquiring the ability of reduced dependence on growth factors. Similarly, exposures of cells to NNK solely for 5 cycles resulted in a detectable increase of cell clones acquiring the ability of reduced dependence on growth factors, and 10 and 15 cycles of exposure resulted in significant and progressive, but additional exposures to NNK for a total of 20 cycles did not result in any significant additional increases of cell clones acquiring the ability of reduced dependence on growth factors. Exposures of cells to B[a]P solely for 5 cycles also resulted in a detectable increase of cell clones acquiring the ability of reduced dependence on growth factors, and additional exposures to B[a]P for a total of 10, 15, and 20 cycles resulted in significant and progressive increases. Comparing the increases of cell clones acquiring the cancer-related ability of reduced dependence on growth factors induced by repeated exposures to individual and combined NNK and B[a]P, we did not detect any synergistic or additive effect of NNK and B[a]P on inducing cells to acquire the ability of reduced dependence on growth factors, though these two distinctive carcinogens were able to induce cellular acquisition of this ability by themselves alone.

To determine whether increased proliferation or increased cell survivability contributed to the increase of survived cell clones acquiring the ability of reduced dependence on growth factors, NB-P10 and -P20 cells were maintained in CM and LM medium for 2, 4, and 6 d. As shown in Figure 1B-1, cell proliferation of NB-P10 and -P20 cells was not higher in

parental MCF10A cells, indicating that cells exposed to NNK and B[a]P did not result in acquisition of increased proliferation. Thus, the increases of cell clones that acquired reduced dependence on growth factors did not result from clone expansion due to increased proliferation. In contrast, NB-P10 and -P20 cells showed higher proliferation rates than parental counterpart cells (Figure 1B-2); in fact, parental MCF10A cells were detectably growth-inhibited. Accordingly, repeated exposures of cells to NNK and B[a]P resulted in acquisition of the cancer-related ability of reduced dependence on growth factors for cell survival and growth.

To determine the tumorigenic ability of NNK- and B[a]P-exposed cells, NB-P10 and -P20 cells were inoculated into nude mice. In contrast to the control breast cancer MCF7 cells, neither NB-P10 nor NB-P20 cells developed any detectable xenograft tumors in 6 mo. Tumorigenicity of these multiclonal cell lines was not detectable; NNK and B[a]P appeared to induce nontumorigenic, precancerous cellular carcinogenesis.

Using the carcinogen-induced progressive acquisition of reduced dependence on growth factors as a biological target endpoint, we have shown the ability of GSPE to suppress NNK-induced precancerous cellular carcinogenesis [16]. Investigating whether GSPE is able to suppress combined NNK- and B[a]P-induced acquisition of reduced dependence on growth factors, we detected that exposure of MCF10A cells to combined NNK and B[a]P in the presence of GSPE, at the maximal noncytotoxic concentration of 40 $\mu\text{g}/\text{mL}$ [16], for 10, 15, and 20 cycles, but not 5 cycles, showed significant reduction of colonies acquiring the ability of reduced dependence on growth factors by 40–50% (Figure 1C), indicating that GSPE was able to suppress the ability of combined NNK and B[a]P in inducing precancerous cellular carcinogenesis with acquisition of reduced dependence on growth factors.

GSPE Suppression of Carcinogen-Induced Acquisition of Anchorage-Independent Growth

Cell adhesion to extracellular matrixes is important for cell survival in a multicell environment; aberrantly increased cell survivability acquired to promote anchorage-independent growth can render cells into tumorigenic transformation [33,34]. As shown in Figure 2A, the acquired ability of anchorage-independent growth was not detectable in NBP5 cells but was detected in NB-P10, -P15, and -P20 cells. Carcinogen exposures for 10 cycles appeared to be required for inducing the acquired ability of anchorage-independent growth; increasing exposures to carcinogens for a total of 15 and 20 cycles progressively increased acquisition of this cancer-related ability, and 15 cycles of exposure to combined NNK and B[a]P appeared to fully induce cells to acquire this ability. Accordingly, acquisition of the ability of anchorage-independent growth appeared to require additional carcinogen exposures (10 cycles) beyond the exposures needed (5 cycles) for acquiring reduced dependence on growth factors.

To measure whether GSPE was able to suppress NNK- and B[a]P-induced acquisition of anchorage-independent growth, we detected that exposure of MCF10A cells to NNK and B[a]P in the presence of GSPE for 10, 15, and 20 cycles, but not 5 cycles, showed significant reduction of colony formation in soft-agar by 35–60% (Figure 2B), indicating the ability of GSPE to suppress cellular acquisition of anchorage-independent growth induced by repeated exposures to combined NNK and B[a]P.

GSPE Suppression of Carcinogen-Induced Acquisition of Acinar-Conformational Disruption

Both acinar structures with a hollow lumen and apicobasally polarized cells are important characteristics found in glandular epithelia in vivo; the disruption of an intact glandular

structure is a hallmark of epithelial cancer, even at its earliest precancerous stages, such as DCIS [26,35,36]. MCF10A cells are able to form acinar structures with a hollow lumen, and apicobasally polarized cells make up these acini on Matrigel [26]. Investigating the potency of combined NNK and B[a]P to induce the precancerous property of acinar-conformational disruption, NB-P5, -P10, -P15, and -P20 cells were seeded on Matrigel for 12 d. As shown in Figure 3A-1, parental MCF10A cells mainly formed regular, round spheroids on Matrigel cultures; NNK- and B[a]P-exposed cells formed both regular and irregular spheroids, and MCF7 cells mainly formed irregular spheroids. Counting the regular and irregular spheroids in these cultures showed significant increases of irregular spheroids associated with the increased exposures to carcinogens for 5 and 10 cycles (Figure 3A-2). Accumulated exposures to NNK and B[a]P for 5 cycles appeared to sufficiently induce MCF10A cells to acquire the precancerous property of acinar-conformational disruption, and 10 cycles of exposures appeared to fully induce cells to acquire this precancerous property. Histological examination revealed a hollow lumen and apicobasal polarization in regular spheroids of MCF10A cells, filling of the luminal space in the irregular spheroids of NNK- and B[a]P-exposed cells (NB-P20), and the loss of apico-basal polarity and filling of the luminal space in the irregular spheroids of MCF7 cells on Matrigel (Figure 3A-3). Although we observed both regular and irregular spheroids of NNK- and B[a]P-exposed cells, we did not detect any spheroids with a hollow lumen by histological examination.

To determine the ability of GSPE to suppress NNK- and B[a]P-induced acquisition of acinar-conformational disruption, exposure of MCF10A cells to NNK and B[a]P in the presence of GSPE for 10, 15, and 20 cycles, but not 5 cycles, showed significant reduction of irregular spheroids on Matrigel by 5–25% (Figure 3B), verifying the ability of GSPE to suppress chronic acquisition of acinar-conformational disruption induced by repeated exposures to combined NNK and B[a]P.

Minimal Effective Doses of GSPE for Suppression of Carcinogenesis

To understand the minimal, effective dose of GSPE required for suppression of NNK- and B[a]P-induced precancerous carcinogenesis, MCF10A cells were exposed to combined NNK and B[a]P in the presence of 40, 10, 2.5, and 0.5 $\mu\text{g}/\text{mL}$ GSPE for 20 cycles. We detected that GSPE at 40, 10, and 2.5 $\mu\text{g}/\text{mL}$, but not at 0.5 $\mu\text{g}/\text{mL}$, significantly suppressed NNK- and B[a]P-increased colony formation in LM medium (Figure 4A), colony formation in soft-agar (Figure 4B), and formation of irregular spheroids on Matrigel (Figure 4C). These data taken together indicated that GSPE suppressed NNK- and B[a]P-induced acquisition of reduced dependence on growth factors, anchorage-independent growth, and acinar-conformational disruption in a dose-dependent manner. GSPE at 2.5 $\mu\text{g}/\text{mL}$ was the minimal, effective dose for suppression of NNK- and B[a]P-induced precancerous carcinogenesis of MCF10A cells.

In addition, GSPE at 40, 10, or 2.5 $\mu\text{g}/\text{mL}$ was not cytotoxic to any of the parental MCF10A and derived NB-P5 to -P20 cells (data not shown). Thus, the mechanism for GSPE to suppress precancerous cellular carcinogenesis induced by NNK and B[a]P was not via induction of cell death or growth inhibition.

Molecular Target Endpoint for GSPE in Suppression of Carcinogenesis

In investigating the molecular target endpoints of GSPE in suppression of precancerous cellular carcinogenesis induced by combined NNK and B[a]P, we used cDNA microarrays and real-time quantitative PCR to detect differentially regulated genes that were changed in carcinogen-exposed cells but whose changes were suppressed in GSPE-protected, carcinogen-exposed cells. Initially, we used cDNA microarrays to study genes whose expressions were consistently changed in target carcinogen-exposed, NB-P10 and NB-P20

cells compared to their counterpart expression levels in reference parent MCF10A cells. After normalization, more than 16 690 genes were detectably expressed in both target and reference cells using SS-H19Kv7 cDNA microarrays. More than 1300 genes were either upregulated or down-regulated in target NB-P10 and -P20 cells more than 1.5-fold over counterpart expression in reference parental MCF10A cells. Filtering with the *t*-test ($P < 0.05$) revealed 68 differentially expressed genes, and subsequent filtering with the Benjamini and Hochberg correction method [37,38] revealed 33 differentially expressed genes. Further filtering revealed eight and two genes were up- and down-regulated, respectively, in NB-P10 and -P20 cells more than twofold over counterpart expression in parental MCF10A cells (Figure 5 and Table 1). Among these 10 genes, 3 genes (FXVD3, HBA2, and HSD11B2) were reportedly related to breast cancer (www.breastcancerdatabase.org [39–42]). Subsequently, we used cDNA microarrays to determine genes whose expressions were changed in NB-P20 cells but whose changes were suppressed in GSPE-protected, NB/GSPE-P20 cells. We detected that the *HSD11B2* gene was upregulated in NB-P20 cells, and its gene expression was protected in NB/GSPE-P20 cells (Table 1).

To investigate whether HSD11B2 gene expression was a molecular target for GSPE in suppression of NNK- and B[a]P-induced precancerous cellular carcinogenesis, we then used RTqPCR measurement and Western immunoblotting with specific antibodies to quantitatively determine whether HSD11B2 gene expression was upregulated in cells exposed to combined NNK and B[a]P and was protected by GSPE. We detected that HSD11B2 gene expression (Figure 6A-1) and protein level (Figure 6A-2) were highly increased up to 154- and 48-fold, respectively, in NNK- and B[a]P-exposed, NB-P20 cells. The increases of gene expression (Figure 6A-1) and protein level (Figure 6A-2) were significantly reduced to fourfold in GSPE-protected, NNK- and B[a]P-exposed, NB/GSPE-P20 cells. These results indicated that increased HSD11B2 expression was likely to be a molecular target endpoint for GSPE in suppression of precancerous cellular carcinogenesis induced by repeated exposure of cells to NNK and B[a]P.

To determine whether increased HSD11B2 expression played an important role in NNK- and B[a]P-induced precancerous cellular carcinogenesis, we used validated siRNAs to knock down the increased HSD11B2 gene expression in NB-P20 cells and studied the effect of the reduced HSD11B2 gene expression on the acquired ability of reduced dependence on growth factors. Transfection of NBP20 cells with validated HSD11B2-specific siRNAs (lane 3), but not control siRNAs (lane 2), resulted in a reduced HSD11B2 protein level (Figure 6B-1) and a significant suppression of the acquired ability of reduced dependence on growth factors (Figure 6B-2). Increased HSD11B2 expression apparently played a contributing role in NNK- and B[a]P-induced cellular acquisition of reduced dependence on growth factors and may serve as a molecular target endpoint for GSPE in suppression of NNK- and B[a]P-induced precancerous cellular carcinogenesis. However, whether increased HSD11B2 expression contributed to cellular acquisition of the cancer-related abilities of anchorage-independent growth and acinar-conformational disruption remains to be determined.

Regulation of Phase I Bioactivating Enzymes in GSPE Suppression of Carcinogenesis

To understand the preventive, noncytotoxic mechanisms for GSPE in suppressing the carcinogenic activity of NNK and B[a]P, we studied gene expression of CYP enzymes in GSPE-induced suppression of NNK- and B[a]P-induced precancerous cellular carcinogenesis. Phase I bio-activating enzymes CYP1A1 and CYP1B1 are postulated to play important roles in activating the carcinogenic activity of NNK and B[a]P [43–53]. We detected that gene expression of CYP1A1 was induced by combined NNK and B[a]P in MCF10A cells in a dose-dependent manner (Figure 7A-1); combined NNK and B[a]P each at 100 pM and 100 nM induced a modest and a high level of CYP1A1, respectively. In contrast, constant gene expression of CYP1B1 was not affected by treatment with NNK and

B[a]P (Figure 7A-1). The increased expression of CYP1A1 was actually induced by B[a]P, but not NNK; treatments of cells with combined or individual NNK and B[a]P at 100 nM showed that gene expression of CYP1A1 was increased up to threefold (Figure 7A-2, lane 2), and the threefold increase was actually induced by B[a]P (lane 4) but not NNK (lane 3).

To understand whether gene expression of CYP1A1 and/or CYP1B1 was modulated by GSPE, we treated cells with GSPE and detected a reduction of both CYP1A1 and CYP1B1 gene expression (Figure 7B). GSPE treatment reduced CYP1A1 gene expression from 1-fold down to 0.5-fold in MCF10A cells (Figure 7B, lanes 1 and 2), from 3-fold down to 2-fold in cells treated with combined NNK and B[a]P (lanes 3 and 4), from 1-fold down to 0.5-fold in NNK-treated cells (lanes 5 and 6), and from 3-fold down to 2-fold in B[a]P-treated cells (lanes 7 and 8). GSPE treatment reduced CYP1B1 gene expression down to 0.5-fold in cells regardless of the treatment with either or both carcinogens at 100 nM (Figure 7B, even lanes). Apparently, gene expression of both CYP1A1 and CYP1B1 was reduced by GSPE treatment.

To further our understanding of the regulation of CYP1A1 in GSPE-induced suppression of cellular carcinogenesis, MCF10A cells were treated with 100 pM B[a]P, which was used to induce chronic precancerous carcinogenesis, in the absence and presence of GSPE. We detected that B[a]P treatment induced an approximately 1.4-fold increase of CYP1A1 gene expression (Figure 7C-1) and protein level (Figure 7C-2, lane 3 vs. lane 1). GSPE treatment induced reduction of CYP1A1 gene expression (Figure 7C-1) and protein level (Figure 7C-2) from 1-fold down to 0.5- and 0.3-fold, respectively, in MCF10A cells (lanes 1 and 2), and reduced CYP1A1 gene expression from 1.4-fold down to 0.8-fold (Figure 7C-1) and protein level from 1.4-fold down to 0.4-fold (Figure 7C-2) in cells cotreated with B[a]P (lanes 3 and 4). Reduction of Phase I bioactivating enzymes CYP1A1 and CYP1B1 was possibly involved in GSPE's ability to suppress NNK- and B[a]P-induced precancerous carcinogenesis via reduction in bio-activation of carcinogens.

In addition, we investigated whether Phase II detoxifying enzymes were involved in GSPE's ability to suppress NNK- and B[a]P-induced precancerous carcinogenesis; however, we did not detect any changes in gene expression of GSTA4, GSTM2, GSTP1, NQO1, and NQO2 [54] induced by GSPE, NNK, or B[a]P (data not shown).

DISCUSSION

Early prevention of human breast cancer associated with chronic exposure to environmental carcinogens by dietary bioactive components is an underinvestigated area. The current challenge in identification of environmental carcinogens in breast cancer development is the low doses of carcinogens involved in transformation of breast cells from noncancerous to precancerous and cancerous stages through a multiyear disease process. Our precancerous carcinogenesis-cellular model mimics chronic carcinogenesis of human breast cells induced by accumulated exposures to environmental carcinogens, and our model is able to reveal the potency of environmental carcinogens at low doses of picomolar ranges to induce cells to acquire cancer-related properties. Although accumulated exposures of noncancerous breast epithelial MCF10A cells to individual [15,16] or combined NNK and B[a]P did not result in transforming cells to acquire the cancerous ability of tumorigenicity, NNK- and B[a]P-exposed cells acquired the cancer-related abilities of reduced dependence on growth factors, anchorage-independent growth, and acinar-conformational disruption. Aberrantly increased cell survivability acquired to reduce a dependence on growth factors and to promote anchorage-independent growth can render cells into tumorigenic transformation [30–34]. Cellular acquisition of acinar-conformational disruption is highly related to breast cells at precancerous stages, such as DCIS, in breast cancer development [26,35,36]. Long-term

exposure to low doses of NNK and B[a]P is conceivable to induce cells entering into a precancerous, but not cancerous, stage in chronic development of human breast cancer. Using the acquired cancer-related properties of reduced dependence on growth factors, anchorage-independent growth, and acinar-conformational disruption as biological target endpoints, we were able to verify the ability of GSPE to suppress precancerous carcinogenesis induced by repeated exposures of cells to NNK and B[a]P in an exposure-and dose-dependent manner. GSPE alone was able to suppress approximately 50% of NNK- and B[a]P-induced precancerous carcinogenic properties as measured by cellular acquisition of cancer-related properties of reduced dependence on growth factors, anchorage-independent growth, and acinar-conformational disruption. Such findings demonstrate that multiple, complementary preventive agents are required to enhance the blockage of NNK- and B[a]P-induced precancerous carcinogenesis. Our working system will continue to provide access to the finding of bioactive components for suppression of precancerous carcinogenesis, leading to identification of agents providing benefits for prevention of breast cancer.

Investigating molecular targets for GSPE in suppression of cellular carcinogenesis, we identified that increased HSD11B2 gene expression served as a molecular target endpoint for GSPE in suppression of NNK- and B[a]P-induced precancerous carcinogenesis. In our previous reports, upregulated gene expression of HSD11B2 was detected in MCF10A cells exposed to either B[a]P [15] or NNK [16]. The upregulated HSD11B2 gene expression in NNK-exposed cells was significantly reduced in cells protected by GSPE [16]. The HSD11B2 gene expression appears to be a common molecular target endpoint of NNK and B[a]P and may also serve as a molecular target endpoint for GSPE in suppression of carcinogen-exposed cells. In this study, we showed that HSD11B2 gene expression and protein level were highly elevated in carcinogen-exposed MCF10A cells acquiring cancer-related properties induced by repeated exposures to both NNK and B[a]P, but the upregulated HSD11B2 levels were significantly reduced in GSPE-protected, carcinogen-exposed cells, as were the acquired cancer-related abilities of reduced dependence on growth factors, anchorage-independent growth, and acinar-conformational disruption. In addition, we furthered our investigation to show that knocking down the upregulated expression in NB-P20 cells with validated HSD11B2-specific siRNAs not only reduced the elevated HSD11B2 protein level but also suppressed the acquired cancer-related ability of reduced dependence on growth factors. Apparently, upregulated HSD11B2 expression played a contributing role in NNK- and B[a]P-induced precancerous cellular carcinogenesis; thus, protection of HSD11B2 gene expression from induction by NNK and B[a]P was important in GSPE suppression of NNK- and B[a]P-induced precancerous carcinogenesis. The human *HSD11B2* gene encodes a 45 kDa protein exhibiting dehydrogenase activity, which is able to deactivate glucocorticoids; expression of HSD11B2 results in inhibition of antiproliferative activity of glucocorticoids [40,41]. Upregulation of HSD11B2 is detected in breast cancer cell lines and breast tumors [40,42], and inhibition of HSD11B2 by glycyrrhetic acid reduces cell proliferation of breast cancer PMC42 cells [42]. Thus, upregulation of HSD11B2 is postulated to play a pro-proliferative role in breast cancer cell growth through suppression of the antiproliferative activity of glucocorticoids [40–42]. However, although HSD11B2 was increased in carcinogen-exposed cells, we did not detect any increased cell proliferation acquired by carcinogen-exposed cells maintained in medium containing hydrocortisol (Figure 1B-1). Accordingly, upregulated HSD11B2 expression may play a novel role in cellular acquisition of cancer-related properties induced by chronic exposure to low doses of environmental carcinogens. Protection of HSD11B2 expression from upregulation may contribute to GSPE's ability to suppress cellular carcinogenesis. However, the mechanisms for HSD11B2 involvement in NNK- and B[a]P-induced precancerous cellular carcinogenesis and in GSPE-induced suppression of cellular carcinogenesis remain to be elucidated.

Studies showed that GSPE inhibits the growth of human breast cancer cells *in culture* [3–5]. In contrast, we did not detect any activity of GSPE at 40 µg/mL to inhibit cell growth or to induce cell death of either parental MCF10A [16] or NNK- and B[a]P-exposed cells; instead, GSPE at noncytotoxic concentrations of 2.5–40 µg/mL was able to reduce NNK- and B[a]P-induced cellular acquisition of cancer-related properties. Studying the preventive, noncytotoxic mechanisms for GSPE in counteracting the carcinogenic activity of NNK and B[a]P, we detected the ability of GSPE to reduce the levels of CYP1A1 and CYP1B1 in MCF10A cells. CYP1A1 and CYP1B1 have been shown to act as bioactivating enzymes for activation of NNK and B[a]P [43–53]. Our finding revealed, for the first time, that GSPE was able to reduce CYP1A1 and CYP1B1 contents in breast cells exposed to NNK and B[a]P. It is possible that reduction of CYP1A1 and CYP1B1 contents may contribute to the ability of GSPE to suppress cellular acquisition of cancer-related properties induced by NNK and B[a]P. However, whether reduction of CYP1A1 and CYP1B1 contents is the noncytotoxic, preventive mechanism for GSPE in suppression of NNK- and B[a]P-induced precancerous cellular carcinogenesis remains to be determined.

Several cell systems have been developed to study cellular carcinogenesis induced by high concentrations of environmental carcinogens. For example, Russo's group used DMBA, B[a]P, methyl-*N*-nitro-nitrosoguanidine, and *N*-methyl-*N*-nitrosourea at micromolar concentrations to induce cellular carcinogenesis of MCF10 cells for studying gene mutations [55,56]. Caruso's group used B[a]P at 1 µM to induce acquisition of anchorage-independent growth and chromosomal alterations, but not tumorigenicity, in MCF10A [23]. Narayan et al. [57] reported that a single-dose treatment of MCF10A cells with cigarette smoke condensate at 1 µg/mL concentration results in acquired anchorage-independent growth. Liu and Lin [58] showed that repeated treatment of MCF10A cells with estrogenic zeranol induces cellular acquisition of anchorage-independent growth and estrogen receptor β gene expression. All these model systems can be used in a preclinical assessment of a potential preventive agent of carcinogenesis associated with occupational exposure to high doses of carcinogens. Our working system presents unique features of low-dose, exposure-dependent chronic carcinogenesis and distinct biological and molecular target endpoints for identifying dietary bioactive components, such as GSPE, and understanding their mechanisms for early prevention of precancerous carcinogenesis in breast cancer induced by repeated exposures to carcinogens at low doses as in environmental exposure. Using this model, we detected that GSPE at concentrations of 2.5–40 µg/mL was able to reduce NNK- and B[a]P-induced cellular acquisition of cancer-related abilities. Applying this cellular model will accelerate the identification of dietary bioactive components for the formulation of combined supplements that can effectively reduce the health risk of human cancers from long-term exposure to carcinogens present in environmental pollution. On the other hand, our model revealed no synergistic nor additive effects of combined use of NNK and B[a]P together on the chronic induction of cellular acquisition of cancer-related properties. Whether long-term exposure of cells to these carcinogens together increases the qualitative complexity, but not the quantitative enhancement, in alterations of genetic and epigenetic machineries in cellular carcinogenesis remains to be studied.

Acknowledgments

We are grateful to Ms. M. Bailey for textual editing of the manuscript. We thank Dr. J. Yuan for his technical assistance in RTqPCR analysis of gene expression, and Dr. S. Newman for her technical assistance in histological examination of spheroid sections. We also thank InterHealth Nutraceuticals for providing GSPE as a gift to our research. This study was initially supported by a grant from the University of Tennessee, College of Veterinary Medicine, Center of Excellence in Livestock Diseases and Human Health (H.-C.R.W.), and was subsequently supported by NIH grant CA125795 (H.-C.R.W.), and a China Scholarship Council scholarship (X.S.).

Abbreviations

GSPE	grape seed proanthocyanidin extract
DCIS	ductal carcinoma in situ
B[a]P	benzo[a]pyrene
NNK	4-(methylnitrosamino)-1-(3-pyridyl)-1-butanone
HSD11B2	hydroxysteroid (11-beta) dehydrogenase 2
CYP1A1	cytochrome P450 1A1
CYP1B1	cytochrome P450 1B1
CM	complete MCF10A medium
LM	lowmitogen
MTT	methyl thiazolyl tetrazolium
RTqPCR	real-time quantitative polymerase chain reaction
TBP	TATA box-binding protein

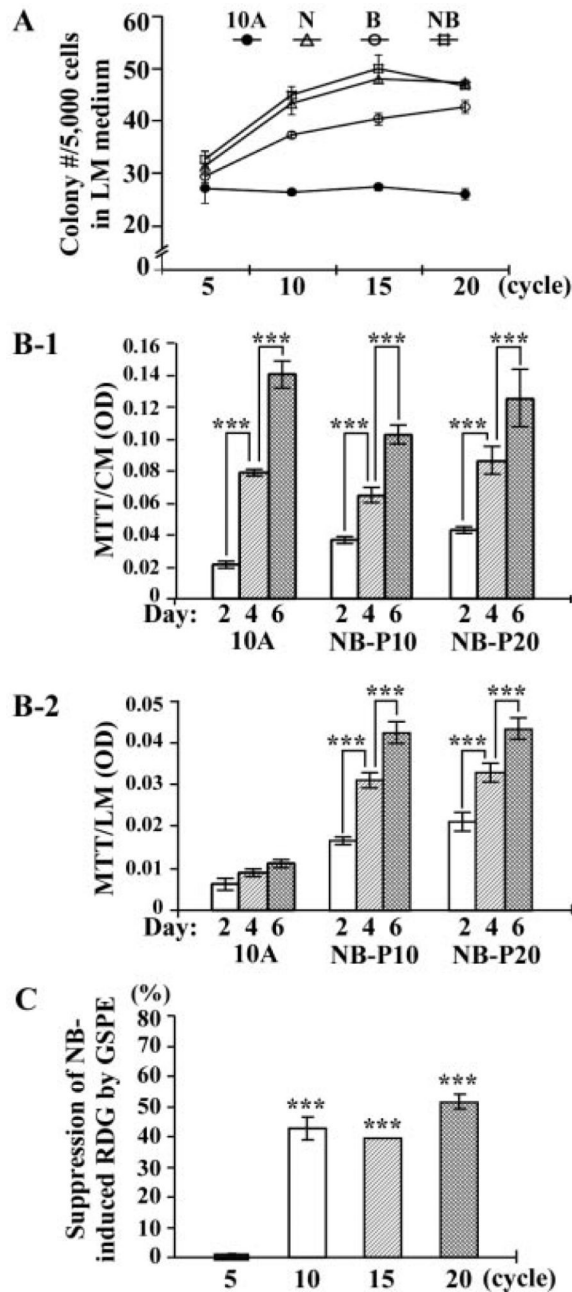
REFERENCES

1. Mehta RG. Experimental basis for the prevention of breast cancer. *Eur J Cancer*. 2000; 36:1275–1282. [PubMed: 10882866]
2. Cos P, De Bruyne T, Hermans N, Apers S, Berghe DV, Vlietinck AJ. Proanthocyanidins in health care: Current and new trends. *Curr Med Chem*. 2004; 11:1345–1359. [PubMed: 15134524]
3. Ye X, Krohn RL, Liu W, et al. The cytotoxic effects of a novel IH636 grape seed proanthocyanidin extract on cultured human cancer cells. *Mol Cell Biochem*. 1999; 196:99–108. [PubMed: 10448908]
4. Bagchi D, Bagchi M, Stohs S, Ray SD, Sen CK, Preuss HG. Cellular protection with proanthocyanidins derived from grape seeds. *Ann N Y Acad Sci*. 2002; 957:260–270. [PubMed: 12074978]
5. Sharma G, Tyagi AK, Singh RP, Chan DC, Agarwal R. Synergistic anti-cancer effects of grape seed extract and conventional cytotoxic agent doxorubicin against human breast carcinoma cells. *Breast Cancer Res Treat*. 2004; 85:1–12. [PubMed: 15039593]
6. Kim H, Hall P, Smith M, et al. Chemoprevention by grape seed extract and genistein in carcinogen-induced mammary cancer in rats is diet dependent. *J Nutr*. 2004; 134:3445S–3452S. [PubMed: 15570052]
7. Guengerich FP. Metabolism of chemical carcinogens. *Carcinogenesis*. 2000; 21:345–351. [PubMed: 10688854]
8. Reynolds P, Hurley S, Goldberg DE, et al. Active smoking, household passive smoking, and breast cancer: Evidence from the California Teachers Study. *J Natl Cancer Inst*. 2004; 96:29–37. [PubMed: 14709736]
9. Hecht SS. Tobacco smoke carcinogens and breast cancer. *Environ Mol Mutagen*. 2002; 39:119–126. [PubMed: 11921179]
10. DeBruin LS, Joseph PD. Perspectives on the chemical etiology of breast cancer. *Environ Health Perspect*. 2002; 110:119–128. [PubMed: 11834470]
11. Li D, Zhang W, Sahin AA, Hittelman WN. DNA adducts in normal tissue adjacent to breast cancer: A review. *Cancer Detect Prev*. 1999; 23:454–462. [PubMed: 10571655]
12. O'Shaughnessy JA, Kelloff GJ, Gordon GB, et al. Treatment and prevention of intraepithelial neoplasia: An important target for accelerated new agent development. *Clin Cancer Res*. 2002; 8:314–346. [PubMed: 11839647]

13. Sanders ME, Schuyler PA, Dupont WD, Page DL. The natural history of low-grade ductal carcinoma in situ of the breast in women treated by biopsy only revealed over 30 years of long-term follow-up. *Cancer*. 2005; 103:2481–2484. [PubMed: 15884091]
14. Mei J, Hu H, McEntee M, Plummer H III, Song P, Wang HC. Transformation of non-cancerous human breast epithelial cell line MCF10A by the tobacco-specific carcinogen NNK. *Breast Cancer Res Treat*. 2003; 79:95–105. [PubMed: 12779086]
15. Siriwardhana N, Wang HCR. Precancerous carcinogenesis of human breast epithelial cells by chronic exposure to benzo[a]pyrene. *Mol Carcinogenesis*. 2008; 47:338–348.
16. Siriwardhana N, Choudhary S, Wang HCR. Precancerous model of human breast epithelial cells induced by NNK for prevention. *Breast Cancer Res Treat*. 2008; 109:427–441. [PubMed: 17653854]
17. Hecht SS, Carmella SG, Chen M, et al. Quantitation of urinary metabolites of a tobacco-specific lung carcinogen after smoking cessation. *Cancer Res*. 1999; 59:590–596. [PubMed: 9973205]
18. Besaratinia A, Maas LM, Brouwer EM, et al. A molecular dosimetry approach to assess human exposure to environmental tobacco smoke in pubs. *Carcinogenesis*. 2002; 23:1171–1176. [PubMed: 12117775]
19. Obana H, Hori S, Kashimoto T, Kunita N. Polycyclic aromatic hydrocarbons in human fat and liver. *Bull Environ Contam Toxicol*. 1981; 27:23–27. [PubMed: 7296033]
20. Rundle A, Tang D, Zhou J, Cho S, Perera F. The relationship between genetic damage from polycyclic aromatic hydrocarbons in breast tissue and breast cancer. *Carcinogenesis*. 2000; 21:1281–1289. [PubMed: 10874004]
21. Rubin H. Synergistic mechanisms in carcinogenesis by polycyclic aromatic hydrocarbons and by tobacco smoke: A bio-historical perspective with updates. *Carcinogenesis*. 2001; 22:1903–1930. [PubMed: 11751421]
22. Cavalieri E, Rogan E, Sinha D. Carcinogenicity of aromatic hydrocarbons directly applied to rat mammary gland. *J Cancer Res Clin Oncol*. 1988; 114:3–9. [PubMed: 3350839]
23. Caruso JA, Reiners JJ Jr, Emond J, et al. Genetic alteration of chromosome 8 is a common feature of human mammary epithelial cell lines transformed in vitro with benzo[a]pyrene. *Mutat Res*. 2001; 473:85–99. [PubMed: 11166028]
24. Chhabra SK, Anderson LM, Perella C, et al. Coexposure to ethanol with N-nitrosodimethylamine or 4-(methylnitrosamino)-1-(3-pyridyl)-1-butanone during lactation of rats: Marked increase in O(6)-methylguanine-DNA adducts in maternal mammary gland and in suckling lung and kidney. *Toxicol Appl Pharmacol*. 2000; 169:191–200. [PubMed: 11097872]
25. Soule HD, Maloney TM, Wolman SR, et al. Isolation and characterization of a spontaneously immortalized human breast epithelial cell line, MCF-10. *Cancer Res*. 1990; 50:6075–6086. [PubMed: 1975513]
26. Debnath J, Muthuswamy SK, Brugge JS. Morphogenesis and oncogenesis of MCF-10A mammary epithelial acini grown in three-dimensional basement membrane cultures. *Methods*. 2003; 30:256–268. [PubMed: 12798140]
27. Specht K, Kremer M, Müller U, et al. Identification of cyclin D1 mRNA overexpression in B-cell neoplasias by real-time reverse transcription-PCR of microdissected paraffin sections. *Clin Cancer Res*. 2002; 8:2902–2911. [PubMed: 12231535]
28. Livak KJ, Schmittgen TD. Analysis of relative gene expression data using real-time quantitative PCR and the $2^{-\Delta\Delta CT}$ method. *Methods*. 2001; 23:402–408. [PubMed: 11846609]
29. Yuan JS, Reed A, Chen F, Stewart CN. Statistical analysis of real-time PCR data. *BMC Bioinformatics*. 2006; 7:85. [PubMed: 16504059]
30. Hanahan D, Weinberg RA. The hallmarks of cancer. *Cell*. 2000; 100:57–70. [PubMed: 10647931]
31. Campisi J, Morreo G, Pardee AB. Kinetics of G1 transit following brief starvation for serum factors. *Exp Cell Res*. 1984; 152:459–466. [PubMed: 6373328]
32. Larsson O, Zetterberg A, Engstrom W. Consequences of parental exposure to serum-free medium for progeny cell division. *J Cell Sci*. 1985; 75:259–268. [PubMed: 4044676]
33. Valentijn AJ, Zouq N, Gilmore AP, Anokis. *Biochem Soc Trans*. 2004; 32:421–425. [PubMed: 15157151]

34. Reddig PJ, Juliano RL. Clinging to life: Cell to matrix adhesion and cell survival. *Cancer Metastasis Rev.* 2005; 24:425–439. [PubMed: 16258730]
35. Debnath J, Brugge JS. Modelling glandular epithelial cancers in three-dimensional cultures. *Nat Rev Cancer.* 2005; 5:675–688. [PubMed: 16148884]
36. Nelson CM, Bissell MJ. Modeling dynamic reciprocity: Engineering three-dimensional culture models of breast architecture, function, and neoplastic transformation. *Semin Cancer Biol.* 2005; 15:342–352. [PubMed: 15963732]
37. Benjamini Y, Hochberg Y. Controlling the false discovery rate: A practical and powerful approach to multiple testing. *J R Stat Soc Ser B.* 1995; 57:289–300.
38. Reiner A, Yekutieli D, Benjamini Y. Identifying differentially expressed genes using false discovery rate controlling procedures. *Bioinformatics.* 2003; 19:368–375. [PubMed: 12584122]
39. Yamamoto H, Okumura K, Toshima S, et al. FXYD3 protein involved in tumor cell proliferation is overproduced in human breast cancer tissues. *Biol Pharm Bull.* 2009; 32:1148–1154. [PubMed: 19571376]
40. Rabbitt EH, Gittoes NJ, Stewart PM, Hewison M. 11Beta-hydroxysteroid dehydrogenases, cell proliferation and malignancy. *J Steroid Biochem Mol Biol.* 2003; 85:415–421. [PubMed: 12943730]
41. Lipka C, Mankertz J, Fromm M, et al. Impairment of the antiproliferative effect of glucocorticosteroids by 11beta-hydroxysteroid dehydrogenase type 2 overexpression in MCF-7 breast-cancer cells. *Horm Metab Res.* 2004; 36:437–444. [PubMed: 15305225]
42. Koyama K, Myles K, Smith R, Krozowski Z. Expression of the 11beta-hydroxysteroid dehydrogenase type II enzyme in breast tumors and modulation of activity and cell growth in PMC42 cells. *J Steroid Biochem Mol Biol.* 2001; 76:153–159. [PubMed: 11384873]
43. Smith TJ, Guo Z, Gonzalez FJ, Guengerich FP, Stoner GD, Yang CS. Metabolism of 4-(methylnitrosamino)-1-(3-pyridyl)-1-butanone in human lung and liver microsomes and cytochromes P-450 expressed in hepatoma cells. *Cancer Res.* 1992; 52:1757–1763. [PubMed: 1312898]
44. Smith TJ, Stoner GD, Yang CS. Activation of 4-(methylnitrosamino)-1-(3-pyridyl)-1-butanone (NNK) in human lung microsomes by cytochromes P450, lipoxygenase, and hydro-peroxides. *Cancer Res.* 1995; 55:5566–5573. [PubMed: 7585636]
45. Fujita K, Kamataki T. Predicting the mutagenicity of tobacco-related N-nitrosamines in humans using 11 strains of *Salmonella typhimurium* YG7108, each coexpressing a form of human cytochrome P450 along with NADPH-cytochrome P450 reductase. *Environ Mol Mutagen.* 2001; 38:339–346. [PubMed: 11774366]
46. Huang Z, Fasco MJ, Figge HL, Keyomarsi K, Kaminsky LS. Expression of cytochromes P450 in human breast tissue and tumors. *Drug Metab Dispos.* 1996; 24:899–905. [PubMed: 8869826]
47. Shimada T, Hayes CL, Yamazaki H, et al. Activation of chemically diverse procarcinogens by human cytochrome P-450 1B1. *Cancer Res.* 1996; 56:2979–2984. [PubMed: 8674051]
48. Shimada T, Oda Y, Gillam EM, Guengerich FP, Inoue K. Metabolic activation of polycyclic aromatic hydrocarbons and other procarcinogens by cytochromes P450 1A1 and P450 1B1 allelic variants and other human cytochromes P450 in *Salmonella typhimurium* NM2009. *Drug Metab Dispos.* 2001; 29:1176–1182. [PubMed: 11502724]
49. Nebert DW, Dalton TP, Okey AB, Gonzalez FJ. Role of aryl hydrocarbon receptor-mediated induction of the CYP1 enzymes in environmental toxicity and cancer. *J Biol Chem.* 2004; 279:23847–23850. [PubMed: 15028720]
50. Baird WM, Hooven LA, Mahadevan B. Carcinogenic polycyclic aromatic hydrocarbon-DNA adducts and mechanism of action. *Environ Mol Mutagen.* 2005; 45:106–114. [PubMed: 15688365]
51. Hughes D, Gattenplan JB, Marcus CB, Subbaramaiah K, Dannenberg AJ. Heat shock protein 90 inhibitors suppress aryl hydrocarbon receptor-mediated activation of CYP1A1 and CYP1B1 transcription and DNA adduct formation. *Cancer Prev Res.* 2008; 1:485–493.
52. Ciolino HP, Yeh GC. Inhibition of aryl hydrocarbon-induced cytochrome P-450 1A1 enzyme activity and CYP1A1 expression by resveratrol. *Mol Pharmacol.* 1999; 56:760–767. [PubMed: 10496959]

53. Kim JH, Stansbury KH, Walker NJ, Trush MA, Strickland PT, Sutter TR. Metabolism of benzo[a]pyrene and benzo[a]pyrene-7,8-diol by human cytochrome P450 1B1. *Carcinogenesis*. 1998; 19:1847–1853. [PubMed: 9806168]
54. Iyanagi T. Molecular mechanism of phase I and phase II drug-metabolizing enzymes: Implications for detoxification. *Int Rev Cytol*. 2007; 260:35–112. [PubMed: 17482904]
55. Russo J, Calaf G, Russo IH. A critical approach to the malignant transformation of human breast epithelial cells with chemical carcinogens. *Crit Rev Oncog*. 1993; 4:403–417. [PubMed: 8353140]
56. Calaf G, Russo J. Transformation of human breast epithelial cells by chemical carcinogens. *Carcinogenesis*. 1993; 14:483–492. [PubMed: 8453725]
57. Narayan S, Jaiswal AS, Kang D, Srivastava P, Das GM, Gairola CG. Cigarette smoke condensate-induced transformation of normal human breast epithelial cells in vitro. *Oncogene*. 2004; 23:5880–5889. [PubMed: 15208684]
58. Liu S, Lin YC. Transformation of MCF-10A human breast epithelial cells by zerenol and estradiol-17beta. *Breast J*. 2004; 10:514–521. [PubMed: 15569208]

**Figure 1.**

GSPE-induced suppression of reduced dependence of growth factors (RDG). (A) MCF10A cultures were exposed to individual (N, B) or combined (NB) NNK and B[a]P each at 100 pM for 5, 10, 15, and 20 cycles. 5×10^3 cells were placed in 100 mm culture dishes and maintained in LM medium for 10 d. Cell colonies (≥ 0.5 mm diameter) were stained with Coomassie brilliant blue and counted. Each value represents a mean of triplicates, and error bars represent standard deviation. Cells exposed to combined NNK and B[a]P each at 100 pM for 5, 10, 15, and 20 cycles resulted in cell lines NB-P5, -P10, -P15, and -P20, respectively. (B-1 and B-2) 5×10^3 cells of parental MCF10A, NB-P10, and NB-P20 were seeded in each well of 96-well plates. After 16 h, cultures were replaced with either (B-1) CM medium or (B-2) LM medium for 2, 4, and 6 d. Quantification of cell viability was

determined by using the MTT assay and measured with an ELISA reader at OD 570 nm. Each value represents a mean of tetraplicates, and error bars represent standard deviation. (C) MCF10A cultures were exposed to combined NNK and B[a]P (NB) each at 100 pM in the presence of 40 µg/mL of GSPE (NB/GSPE) for 5, 10, 15, and 20 cycles. Cells were then seeded and maintained in LM medium for 10 d. Cell colonies (≥0.5 mm diameter) were stained with Coomassie brilliant blue and counted. The value of the suppression effectivity of GSPE on carcinogenesis was calculated by $\{1 - (\# \text{ of NB/GSPE-induced cell colonies}) - (\# \text{ of MCF10A cell clones})\} \div [(\# \text{ of NB-induced cell clones}) - (\# \text{ of MCF10A cell colonies})] \times 100 (\%)$. Each value represents a mean of triplicates, and error bars represent standard deviation. The Student's *t*-test was used to analyze statistical significance, indicated by *** $P < 0.001$. All results are representative of at least two independent experiments.

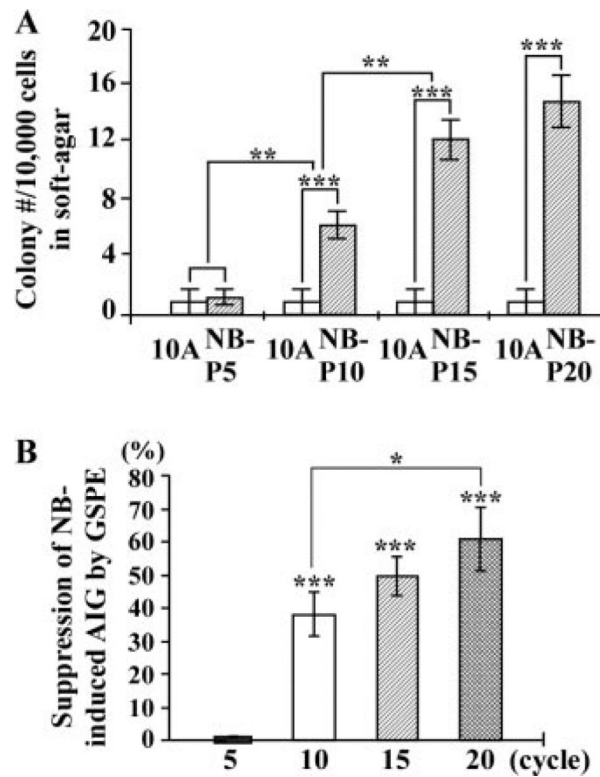
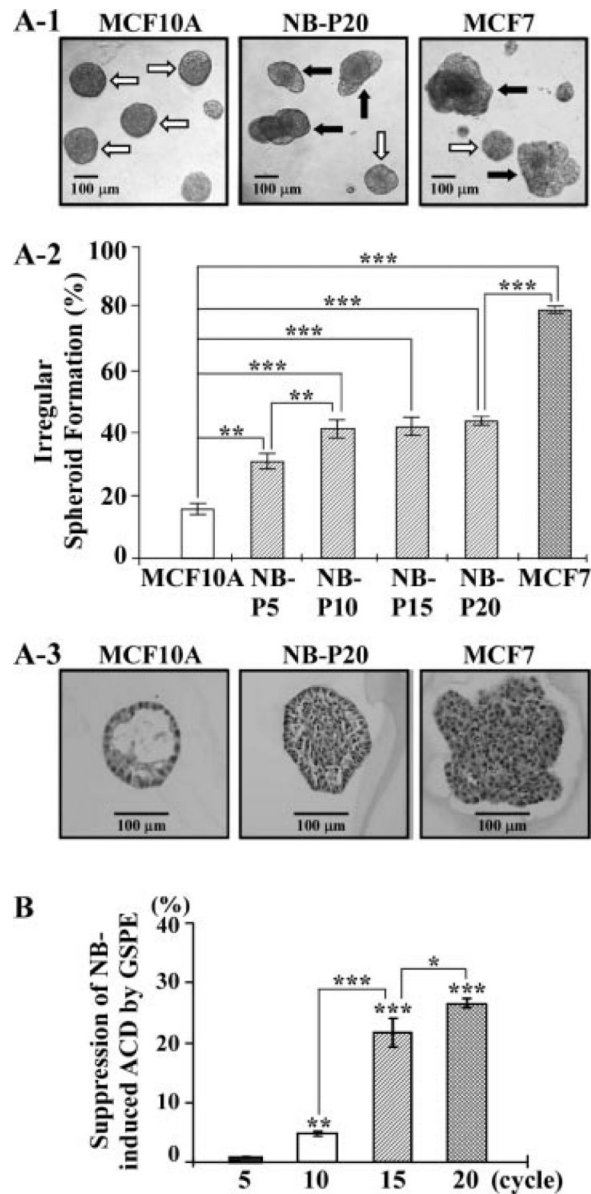


Figure 2.

GSPE-induced suppression of anchorage-independent growth (AIG). (A) 1×10^4 parental MCF10A, NB-P5, NB-P10, NB-P15, and NB-P20 cells were seeded in soft-agar for 20 d, and cell colonies (≥ 0.1 mm diameter) were counted. (B) MCF10A cultures were exposed to combined NNK and B[a]P (NB) each at 100 pM in the presence of 40 $\mu\text{g}/\text{mL}$ of GSPE for 5, 10, 15, and 20 cycles. 1×10^4 cells were seeded in soft-agar for 20 d, and cell colonies (≥ 0.1 mm diameter) were counted. The value of the suppression effectivity of GSPE on carcinogenesis was calculated by $\{1 - [(\# \text{ of NB/GSPE-induced cell colonies}) - (\# \text{ of MCF10A cell clones})] \div [(\# \text{ of NB-induced cell clones}) - (\# \text{ of MCF10A cell clones})]\} \times 100$ (%). Each value represents a mean of triplicates, and error bars represent standard deviation. The Student's *t*-test was used to analyze statistical significance, indicated by * $P < 0.05$, ** $P < 0.01$, *** $P < 0.001$. All results are representative of at least two independent experiments.

**Figure 3.**

GSPE-induced suppression of acinar-conformational disruption (ACD). 2×10^3 parental MCF10A, NB-P5, NB-P10, NB-P15, NB-P20, and breast cancer MCF7 cells were seeded on Matrigel in wells of a 24-well culture plate and maintained for 12 d. (A-1) Regular, round spheroids (white arrow) and irregular spheroids (black arrow) were developed in cultures of parental MCF10A, NB-P20, and MCF7 cells. (A-2) Regular and irregular spheroids in each culture were counted, and the percentage of irregular spheroids in each culture was calculated. Each value represents a mean of triplicates, and error bars represent standard deviation; the Student's *t*-test was used to analyze statistical significance, indicated by ** $P < 0.01$, *** $P < 0.001$. (A-3) Typical spheroids on Matrigel were isolated for histological examination to reveal a hollow lumen and apicobasal polarization in a regular spheroid of MCF10A cells, filling of the luminal space in a spheroid of NB-P20 cells, and the loss of apicobasal polarity and filling of the luminal space in an irregular spheroid of MCF7 cells. Bars indicate 100 μm . All results are representative of at least three independent experiments

(A-1 to A-3). (B) MCF10A cultures were exposed to combined NNK and B[a]P (NB) each at 100 pM in the presence of 40 µg/mL of GSPE for 5, 10, 15, and 20 cycles. Cells were then seeded on Matrigel. Numbers of regular and irregular spheroids in each Matrigel culture were counted; then, the percentage of irregular spheroids in each culture was calculated. The value of the suppression effectivity of GSPE on carcinogen-induced formation of irregular spheroids was calculated by $\{[(\% \text{ of NB-induced irregular spheroid population}) - (\% \text{ of NB/GSPE-induced irregular spheroid population})] \div [(\% \text{ of NB-induced irregular spheroid population}) - (\% \text{ of irregular spheroid population in MCF10A cultures})]\} \times 100 (\%)$. Each value represents a mean of triplicates, and error bars represent standard deviation; the Student's *t*-test was used to analyze statistical significance, indicated by **P* < 0.05, ***P* < 0.01, ****P* < 0.001. The result is representative of two independent experiments.

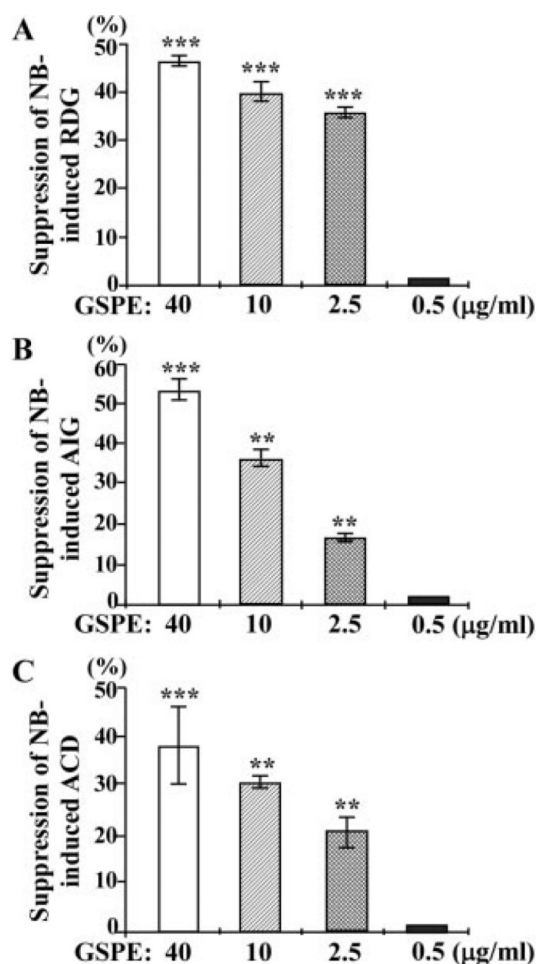


Figure 4. Minimal effective doses of GSPE for suppression of NNK- and B[a]P-induced carcinogenic properties. MCF10A cultures were repeatedly exposed to combined NNK and B[a]P (NB) each at 100 pM in the presence of 40, 10, 2.5, and 0.5 µg/mL of GSPE (NB/GSPE) for 10 and 20 cycles. (A) To detect suppression effectivity of GSPE on cellular acquisition of reduced dependence on growth factors (RDG), cells were seeded and maintained in LM medium for 10 d. Cell colonies (≥ 0.5 mm diameter) were stained with Coomassie brilliant blue and counted. (B) To detect suppression effectivity of GSPE on cellular acquisition of anchorage-independent growth (AIG), cells were seeded in soft-agar for 20 d. Cell colonies (≥ 0.1 mm diameter) were counted. (A and B) The value of the suppression effectivity of GSPE on carcinogenesis was calculated by $\{1 - [(\# \text{ of NB/GSPE-induced cell colonies}) - (\# \text{ of MCF10A cell clones})] \div [(\# \text{ of NB-induced cell clones}) - (\# \text{ of MCF10A cell clones})]\} \times 100$ (%). (C) To detect suppression effectivity of GSPE on cellular acquisition of acinar-conformational disruption (ACD), cells were seeded on Matrigel. Numbers of regular and irregular spheroids in each Matrigel culture were counted; then, the percentage of irregular spheroids in each culture was calculated. The value of the suppression effectivity of GSPE on carcinogen-induced formation of irregular spheroids was calculated by $\{[(\% \text{ of NB-induced irregular spheroid population}) - (\% \text{ of NB/GSPE-induced irregular spheroid population})] \div [(\% \text{ of NB-induced irregular spheroid population}) - (\% \text{ of irregular spheroid population in MCF10A cultures})]\} \times 100$ (%). Each value represents a mean of triplicates, and error bars represent standard deviation. The Student's *t*-test was used to analyze

statistical significance, indicated by $**P < 0.01$, $***P < 0.001$. All results are representative of at least two independent experiments.

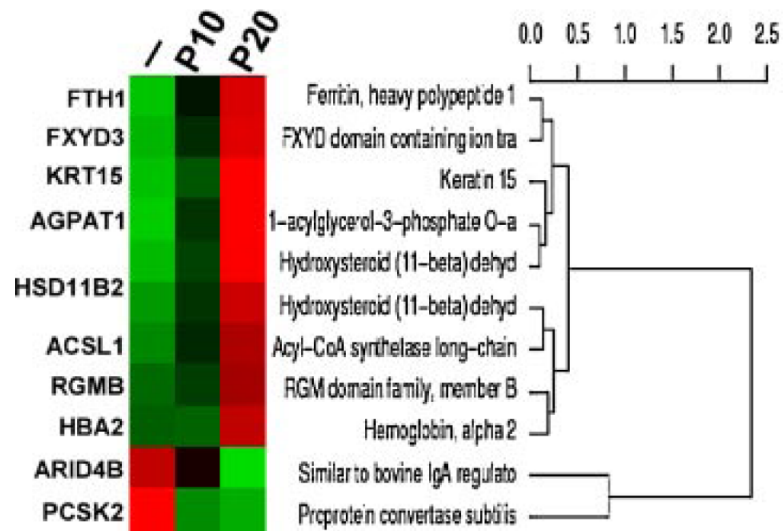


Figure 5. Hierarchical cluster of differentially expressed genes associated with carcinogenesis induced by combined NNK and B[a]P. Total RNAs were isolated from reference vector-treated MCF10A (-) and target NB-P10 (P10) and NB-P20 (P20) cells to detect differentially expressed genes in target cells using human 19K-EST microarrays. Differentially regulated genes were manifested by hierarchical clustering. [Color figure can be viewed in the online issue, which is available at www.interscience.wiley.com.]

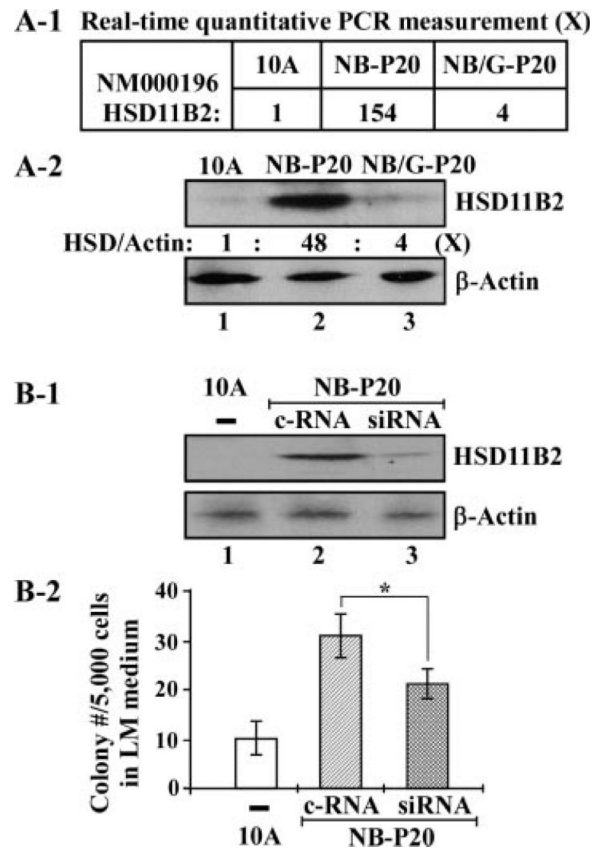
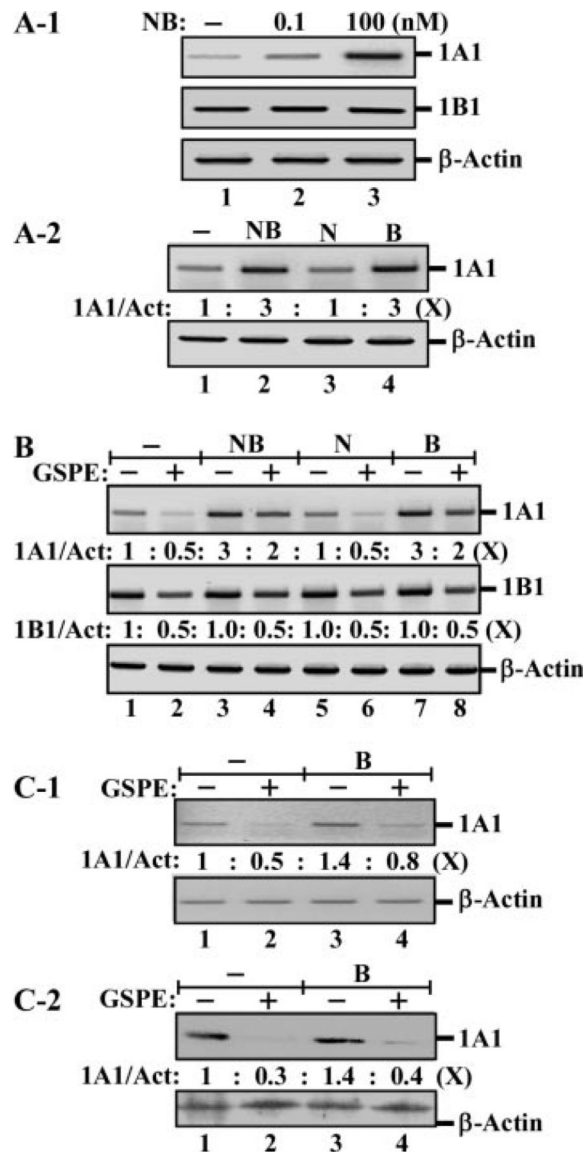


Figure 6. HSD11B2 as a molecular target for GSPE in suppression of cellular carcinogenesis. (A-1) Total RNAs were isolated from parental MCF10A, NB-P20, and NB/GSPE-P20 (NB/G-P20) cells. Gene expression of *HSD11B2* was measured with RTqPCR to determine the relative gene expression levels in NB-P20 and NB/GSPE-P20 cells versus their counterpart gene expression in parental MCF10A cells. (A-2) Whole cell lysates were prepared from parental MCF10A, NB-P20, and NB/GSPE-P20 cells and analyzed by Western immunoblotting using specific antibodies to detect levels of HSD11B2, with β -actin as a control. Levels of HSD11B2 and β -actin were quantified by densitometry. The relative protein levels of HSD11B2 (HSD/actin) were calculated by normalizing the levels of HSD11B2 with the levels of β -actin and then normalized by the level in parental MCF10A cells (lane 1), set as 1 (X, arbitrary unit). (B-1 and B-2) NB-P20 cells were transfected with control siRNAs (c-RNA) or validated, HSD11B2-specific siRNAs (siRNA) for 64 h. (B-1) Whole cell lysates of parental MCF10A (10A) and transfected NB-P20 cells were prepared and analyzed by Western immunoblotting using specific antibodies to detect levels of HSD11B2, with β -actin as a control. (B-2) 5×10^3 parental MCF10A (10A) and transfected NB-P20 cells were seeded in 100 mm culture dishes and maintained in LM medium for 10 d. Cell colonies grown in LM medium (≥ 0.5 mm diameter) were stained with Coomassie brilliant blue and counted. Each value represents a mean of triplicates, and error bars represent standard deviation. The Student's *t*-test was used to analyze statistical significance, indicated by $*P < 0.05$. All results are representative of two independent experiments.

**Figure 7.**

Regulation of bioactivating enzymes by carcinogens and GSPE. (A-1) MCF10A cultures were treated with combined NNK and B[a]P (NB) each at 0, 0.1, and 100 nM for 48 h. (A-2) MCF10A cultures were treated with combined NNK and B[a]P (NB), NNK (N), or B[a]P (B) each at 100 nM for 48 h. (B) MCF10A cultures were treated with combined NNK and B[a]P (NB), NNK (N), or B[a]P (B) each at 100 nM in the absence and presence of 40 μ g/mL GPSE for 48 h. (C-1 and C-2) MCF10A cultures were treated with 100 pM B[a]P (B) in the absence and presence of 40 μ g/mL GPSE for 48 h. (A-1, A-2, B, and C-1) Total RNAs were isolated and analyzed by PCR with specific primers to determine relative gene expression levels of CYP1A1 (1A1) and CYP1B1 (1B1), with β -actin as a control. (A-2, B, and C-1) Total gene expression levels of *CYP1A1*, *CYP1B1*, and β -actin were quantified by densitometry. The relative gene expression levels of *CYP1A1* (1A1/Act) and *CYP1B1* (1B1/Act) were calculated by normalizing the expression levels of *CYP1A1* and *CYP1B1* with the cognate expression levels of β -actin and then normalized by the level in untreated MCF10A cells, set as 1 (X, arbitrary unit). (C-2) Whole cell lysates were prepared and analyzed by Western immunoblotting using specific antibodies to detect levels of CYP1A1, with β -actin

as a control. Levels of CYP1A1 and β -actin were quantified by densitometry, and the relative protein levels of CYP1A1 (1A1/Act) were calculated by normalizing the levels of CYP1A1 with the levels of β -actin and then normalizing by the level in untreated MCF10A cells (lane 1), set as 1 (X, arbitrary unit). All results are representative of two (A-1, A-2, and B) or three (C-1 and C-2) independent experiments.

Table 1

Differentially Regulated Genes and Molecular Target Endpoints

Genes differentially regulated commonly in NB-P10 and -P20 cells	Molecular target endpoints for GSPE
Eight upregulated genes	
<i>ACSL1</i> : acyl-CoA synthetase long-chain family member 1	—
<i>AGPAT1</i> : 1-acylglycerol-3-phosphate-O-acyltransferase 1	—
<i>FTH1</i> : ferritin, heavy polypeptide 1	—
<i>FXRD3</i> : FXRD domain containing ion transport regulator 3	—
<i>HBA2</i> : hemoglobin alpha 2	—
<i>HSD11B2</i> : hydroxysteroid (11-beta) dehydrogenase 2	↓
<i>KRT15</i> : keratin 15	—
<i>RGMB</i> : RGM domain family member B	—
Two downregulated genes	
<i>ARID4B</i> : similar to bovine IgA regulator	—
<i>PCSK2</i> : proprotein convertase subunit 2	—

↓, downregulated by GSPE; —, no change.